Audio Engineering Society

Convention Paper

Presented at the 129th Convention
2010 November 4–7 San Francisco, CA, USA

The papers at this Convention have been selected on the basis of a submitted abstract and extended precis that have been peer reviewed by at least two qualified anonymous reviewers. This convention paper has been reproduced from the author's advance manuscript, without editing, corrections, or consideration by the Review Board. The AES takes no responsibility for the contents. Additional papers may be obtained by sending request and remittance to Audio Engineering Society, 60 East 42nd Street, New York, New York 10165-2520, USA; also see www.aes.org. All rights reserved. Reproduction of this paper, or any portion thereof, is not permitted without direct permission from the Journal of the Audio Engineering Society.

Measures and parameter estimation of triodes, for the real-time simulation of a multi-stage guitar preamplifier

Ivan Cohen[1] [2], and Thomas Helie [1]

[1] *Ircam - CNRS - STMS UMR 9912, Analysis/Synthesis Team, Paris, France*

[2] *Orosys R&D, Montpellier, France*

Correspondence should be addressed to Ivan Cohen, Thomas Helie (ivan.cohen@orosys.fr, thomas.helie@ircam.fr)

ABSTRACT

This paper deals with the real-time simulation of a multi-stage guitar preamplifier. Dynamic triode models based on Norman Korens model, and "secondary phenomena" as grid rectification effect and parasitic capacitances are considered. Then, the circuit is modeled by a nonlinear differential algebraic system, with extended state-space representations. Standard numerical schemes yield efficient stable simulations of the circuit, and are implemented as VST plug-ins. Measures of real triodes have been realized, to develop new triode models, and to characterize the capabilities of aged and new triodes. The results are compared for all the models, using lookup tables generated with the measures, and Norman Korens model with its parameters estimated from the measures.

1. INTRODUCTION

Many commercial guitar amplifiers simulations have been released today, and several papers about this subject have been published [2, 3, 5, 13, 14]. They are often focused on common cathode triode amplifier modeling, a circuit widely used in guitar and hi-fi amplifiers to increase the voltage amplitude of a sound signal. A triode model is chosen, as the one from Norman Koren [3]. This model matches well with the triode behaviour displayed in the datasheets. Nevertheless, some phenomena as grid rectification effect or parasitic capacitances, and accuracy between models and real triodes, are rarely described. Moreover, in simulations, the interaction

between multiple stages is usually not studied.

In this article, we want to study and simulate in real time a simplified vacuum tube guitar preamplifier. It is made of two common cathode triode amplifiers (see figure 7), and a typical guitar amplifier tone stack (figure 9). In section 2, the Norman Korens triode model is considered. We suggest different ways to improve its accuracy, based on a precedent work (see [1]), and measures of real triodes (section 3). They are realized on 12AX7 with different capabilities, using look-up tables (i) and identification algorithms (ii). Numerical schemes are suggested in section 4, using extended state space representations, and methods to resolve system of differential algebraic equations. Then, the stages of a preamplifier are studied in section 5. The influence of the coupling between them is displayed. The results are compared with the behaviour of a simplified topology, without real coupling, but less CPU consuming. Finally, these models are simulated in real-time.

Sound examples are available at `http://www.orosys.fr/cohen/aes129.htm`.

2. PARAMETRIZED MODELS OF TRIODES

The triode is a vacuum tube, with three pins : the grid (G), the cathode (K) and the plate (P). The indirectly heated cathode causes a space charge of electrons that may be attracted to the positively charged plate, and creates a current. Then, a negative voltage is applied to the grid to control the amount of electrons repelled back towards the cathode. This electronic component has a strongly nonlinear behaviour in the working area we consider. Its model is very important for the realism of the complete stage's simulation.

We consider the triode equivalent to two current sources I_g and I_p, dependant on the voltages V_{gk} (grid-cathode) and V_{pk} (plate-cathode). These currents are always positive, around a few mA. The influence of the heater is neglected.

The vacumm tube guitar preamplifiers use almost systematically 12AX7 dual triodes (also called ECC83). This is a "high gain" triode, its gain parameter μ being around 100.

2.1. (Basic) Norman Koren's model

Derived from the Leach model, Norman Koren's model is "phenomenological", and models the behavior of physical phenomena using parameters not derived from fundamental physics. It has been designed so that plate current $I_p > 0$ whenever plate voltage $V_{pk} > 0$ [3]. It matches better published curves from datasheets. The expression of the I_p current is the following :

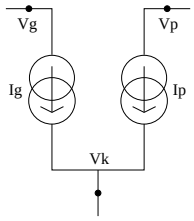

Fig. 1: The triode's model

$$I_p = \frac{E_1^{E_x}}{K_g}(1 + \mathrm{sgn}(E_1)) \tag{1}$$

with :

$$E_1 = \frac{V_{pk}}{K_p} \ln\left[1 + \exp\left(K_p\left(\frac{1}{\mu} + \frac{V_{gk} + V_{ct}}{\sqrt{K_{vb} + V_{pk}^2}}\right)\right)\right]$$

Typical parameters values from [3] and SPICE models are displayed in the table 1.

μ	E_x	K_g	K_p	V_{ct}	K_{vb}
100	1.4	1060	600	0	300

Table 1: Norman Koren's typical parameters values

2.2. Grid rectification effect

The I_g current is responsible for the grid rectification effect that designers try to contain using specific polarizations and a resistance in front of the triode's grid. When the grid-to-cathode voltage V_{gk} becomes positive, the value of I_g increases by a few mA. As a result, the voltage measured at the grid is limited in its positive course. The triode acts like a rectifier. This kind of distortion is not wanted by electronic designers, but exists for high gain configurations. It is one of the causes of plate voltage's saturation [1], and a phenomenon that differentiates the behaviour of vacuum tubes from the transistors [8].

In [1], the grid current model was a simple approximation of a diode's characteristic. A smooth transition is added between the resistive behaviour and the

interval of voltages where the current is null, with a second order polynomial. This model gives results close to SPICE's diode models and the measures we have done as we will see later.

$$I_g = \begin{cases} 0 & \text{if } V_{gk} < V_\gamma - K_n \\ \frac{V_{gk} - V_\gamma}{R_{gk}} & \text{if } V_{gk} > V_\gamma + K_n \\ aV_{gk}^2 + bV_{gk} + c & \text{otherwise} \end{cases} \quad (2)$$

with

$$\begin{aligned} a &= \frac{1}{4K_n R_{gk}} \\ b &= \frac{K - V_\gamma}{2K_n R_{gk}} \\ c &= -a(V_\gamma - K_n)^2 - b(V_\gamma - K_n) \end{aligned} \quad (3)$$

The parameter R_{gk} controls the resistive behaviour of the grid current, V_γ is the voltage threshold between the null and resistive behaviour. The parameter K_n is the length of the smooth transition.

2.3. Parasitic capacitances and Miller effect

The dynamic behaviour of the triode model is considered. Three capacitances are introduced between each pole, with their capacitance values chosen according to the datasheets (around a few picofarads). In spite of their low values, one of them, the capacitance C_{gp} between the grid and the plate, changes the frequency response of a triode circuit below 20 kHz. This is the consequence of the Miller effect. The capacitance acts as its value is multiplied by the gain of the stage (around 60), like a lowpass filter with the resistance in front of the triode's grid. The cutoff frequency is 5 kHz and more. The other capacitances can be neglected (see [1]). These results have been confirmed by SPICE simulations and listening tests.

3. MEASURES OF TRIODES

A device has been developed to measure the static behaviour of different kinds of triodes. Their dynamic behaviour will be studied in a future work.

The results are shown as series of triplets $(I_p, V_{gk}, V_{pk})_i$ and $(I_g, V_{gk}, V_{pk})_i$. The triodes measured are the following : a 12AX7 Sovtek bougth in a music store (1), another 12AX7 recently put in a guitar amplifier (2), and a 12AX7 used for several years in a guitar amplifier (3). At the beginning, we work on the plate current I_p only.

The measured triplets are used in MATLAB to generate a surface $I_p = f(V_{gk}, V_{pk})$ (see figure 2) using bilinear interpolation. The measures cover all the working range of the triode, constrained by the maximum power dissipation and the maximum plate current recommanded in the datasheets (1.5W and 10 mA for the 12AX7). Several methods have been developed to model the real triodes using these measures.

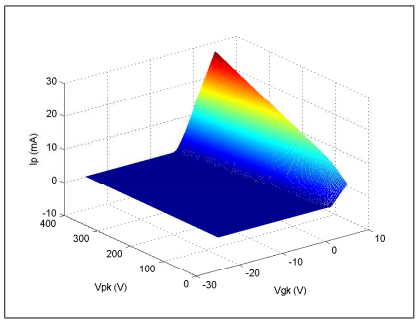

Fig. 2: Characterization surface for the I_p current

3.1. Interpolation

A lookup table of I_p is generated using equally spaced dots of the surface. The voltages are limited to $0 \leq V_{pk} \leq 400$ V and $-10 \leq V_{gk} \leq 5$ V. This table is used in simulation, with a low step, using bilinear or bicubic interpolation to calculate any current value in the limited range, as well as the derivatives [9].

3.2. Identification

Then, the Norman Koren's model is used again, and its parameters are estimated for each measured triode. Let n be the number of measures used for the estimation. Let θ be a vector where Norman Koren's parameters are stored.

$$\theta = [\mu \quad E_x \quad K_g \quad K_p \quad V_{ct} \quad K_{vb}]^T \quad (4)$$

y_i is the I_p current's value from the measure i, and $\hat{Y}_i(\theta)$ the I_p current's value calculated with the parameters θ and the voltages (V_{gk}, V_{pk}) from the measure i. Let $\Phi(\theta)$ the objective function of the least squares, defined as :

$$\Phi(\theta) = \sum_{i=1}^{n} (y_i - \hat{Y}_i(\theta))^2 \quad (5)$$

This function is the optimization criterion, which evaluates the accuracy of the estimation. The function *fminsearch* of MATLAB is used to minimize $\Phi(\theta)$, with the Nelder-Mead's optimization method [10]. It is applied to the 3 test triodes (1) (2) (3) and to some data extracted from a datasheet (4).

The identifiability of Norman Koren's model is checked. The optimization algorithm is tested on the model with realistic parameters (well known), which returns these parameters with an error lower than 1%. Then, the estimation is done with a few measures (n around 10), to get the results of the table 2.

	μ	E_x	K_g	K_p	V_{ct}	K_{vb}
(1)	106	1.46	1572	464	0.49	179
(2)	107	1.46	1551	538	0.52	201
(3)	96	1.39	1408	866	0.29	171
(4)	105	1.53	1934	712	0.67	255

Table 2: Norman Koren's parameters for each 12AX7 triode

3.3. Comparisons between triode's models

We compare the differences between the triodes with the figure 3 and the table 2. The old age of the triode (3) is displayed by a reduction of the gain (μ parameter). Globally, for fixed voltages V_{gk} and V_{pk}, the I_p current will be smaller for an aged triode than for a new one. This observation is used in the aged vacuum tubes detectors. Other parameters as E_x, K_g and V_{ct} are smaller in the triode (3).

In the figure 4, minimal differences between the interpoled model and the estimated model of the triode (1) are shown. We consider two possible causes for these differences. First, the estimation algorithm may be improved, using more measures or other optimization criterion, like weighted or nonlinear least squares. Then, the Norman Koren's viability is considered. This model may be unable to match exactly with a real triode's behaviour. For example, the derivative at the origin of the I_p current with the voltage V_{pk} is null, which is not the case in reality. Some parameters as μ and E_x may not be constant. But our data displays that this model is a quite accurate approximation of a real triode, for the I_p current behaviour.

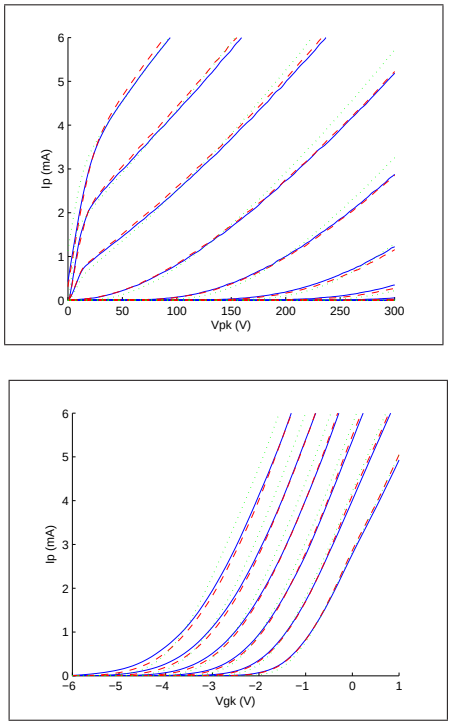

Fig. 3: Interpoled currents from the triode (1), the triode (2), and the triode (3)

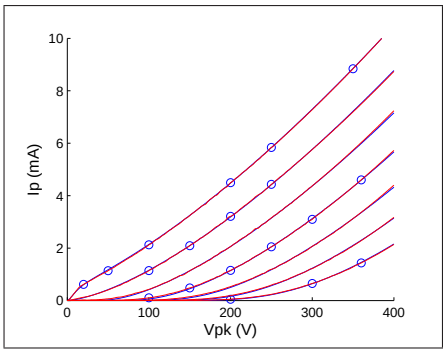

Fig. 4: Estimation using data (circles) and interpolation

3.4. Grid current

We consider again the grid current I_g. The figure 5 displays the grid current's behaviour of the triode (1). These measures show a low dependence on the voltage V_{pk}, so we choose the model from the equation 2 as a good approximation of the measured grid current. Its parameters are estimated and shown in the table 3.

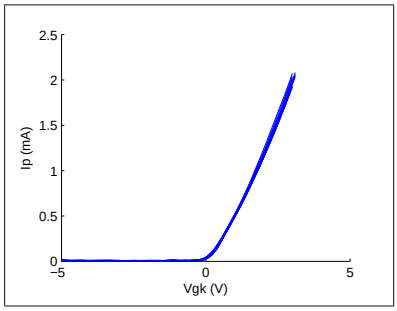

Fig. 5: Grid current measured for several constant values of V_{pk}

	V_γ	R_{gk}	K
new (1)	0.35	1300	0.5
new (2)	0.18	1280	0.49
aged (3)	0.33	1350	0.55

Table 3: Grid current parameters for several 12AX7 triodes

4. NUMERICAL SCHEMES

4.1. Extended State-Space Representations

Linear state-space representations are well known in control engineering. For nonlinear cases, nonlinear functions can be introduced in their classical formulation. Moreover, the nonlinearity can introduce implicit equations. We have suggested an extended state-space representation in [1], to separate the differential equations of implicit problems, with the introduction of a static nonlinear vector W. This is a similar but more general state-space representation for nonlinear systems than the K-method (see [11]). Let X be the dynamic state vector of the studied system, W a static nonlinear state, U the input vector and Y the output vector.

$$dX/dt = f(X,W,U) \quad (6)$$
$$0 = g(X,W,U) \quad (7)$$
$$Y = h(X,W,U) \quad (8)$$

Remark : the linear case is a particular extended state space representation without the function g, with dim $W = 0$ and the functions $f(X,U) = AX + BU$ and $h(X,U) = CX + DU$ (A, B, C and D are constant matrices).

4.2. Discretization

The discretization of the extended state-space equations is done with the resolution of differential and implicit equations. Their complexity is a consequence of the numerical scheme chosen for the resolution, and the existence of nonlinear delay-free loops in the electronic circuit. Let T_e be the sampling period.

4.2.1. Differential equations

To resolve the ordinary differential equations (equation 6), explicit Runge-Kutta methods are often used, because of their good stability and accuracy performances [6], for example the second order method (equation 9). Implicit methods are also used, as backward Euler's method, or trapezoidal method (equation 10), often called bilinear transform and widely used in digital signal processing.

$$k_1 = T_e f(X_n, W_n, U_n) \quad (9)$$
$$X_{n+1} = X_n + T_e f(X_n + \frac{k_1}{2}, W_n, \frac{U_n + U_{n+1}}{2})$$

$$X_{n+1} = X_n + \frac{T_e}{2} f(X_{n+1}, W_{n+1}, U_{n+1}) + \frac{T_e}{2} f(X_n, W_n, U_n) \quad (10)$$

We have seen in [1] that the consideration of the parasitic capacitance C_{gp} in the triode's model makes a stiffness problem appear. There is no rigorous definition of stiffness in the literature, but it can be considered as a differential equation for which certain numerical methods for solving the equation are numerically unstable, with some terms that can lead to rapid variation in the solution. Decreasing the sampling step, and using implicit schemes are two solutions to get rid of the stiff equations. In the first

case, we need sampling frequencies up to some megahertz to get a stable numerical scheme, or variable sampling steps. They are widely used in "offline" simulators (as SPICE), but are not convenient for real time applications. So, implicit methods of differential equations resolution are prefered in stiff numerical schemes.

4.2.2. Implicit equations

The standard method of Newton-Raphson is used to solve implicit equations written $f(Z) = 0$ with Z a vector of any dimension, and find its roots. This algorithm is well known [6], uses the Jacobian matrix $J_f(Z)$ of the function $f(Z)$, and converges to a solution after a specified number of iterations. It is important to check if its application's conditions are satisfied, if the Jacobian matrix is Lipschitz continuous and locally isomorphic around the solution [6]. This is generally the case for our state-space equations. When the interpoled model is used, processing has been done to make sure that the derivatives of the currents I_p and I_g are monotonic.

This method resolves the equation 7 but also the equation 6 if implicit methods of differential equation's resolution are used. So, with the capacitance C_{gp} considered in the equations, Z is the vector $[X \quad W]^T$.

Let Z_n^k be the approximative value of Z at the iteration k of the algorithm for the sample n. $J_f(Z)$ is the Jacobian matrix of $f(Z)$.

$$Z_n^{k+1} = Z_n^k - J_f^{-1}(Z_n^k) \times f(Z_n^k) \qquad (11)$$

5. THE MULTI-STAGE GUITAR PREAMPLIFIER

The circuit we are studying is a simplified guitar preamplifier, made of two common cathode triode amplifiers (A1,A2) and a typical guitar tone stack (T). The triodes chosen by designers are very often 12AX7s. First, each electronic stage is considered separately. Their extended state-space representation is given, and the circuit is simulated using an explicit numerical scheme to show its behaviour. Then, they are interconnected, and the influence of the inter-stage coupling on the preamplifier's harmonic response is discussed.

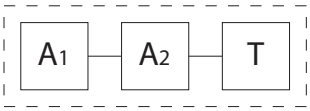

Fig. 6: The vacuum tube guitar preamplifier scheme

5.1. Common cathode triode amplifier

5.1.1. The circuit

The common cathode triode amplifier is a topology of circuit that has been widely used in hi-fi and guitar amplifiers. Easy to design, with a well known behaviour, musicians and audiophiles like its sound properties. So, its use today is justified, several years after the apparition of transistors, as its study in papers about guitar amplifiers simulation [5, 13, 14]. It is found in most of the vacuum tube guitar preamplifiers, which have the purpose to increase the voltage of the guitar's signal (with a maximum voltage of 400 mV, and an impedance of 20 kΩ, depending on the type of guitar pickup), and to enrich its tone.

The circuit is very simple, the triode 12AX7 is connected with a few resistances and two capacitances. We don't consider the parasitic capacitance between the plate and the grid to simplify the extended state-space representation.

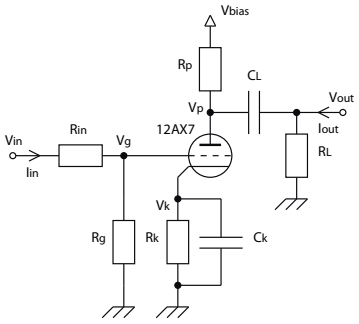

Fig. 7: The Common Cathode Triode Amplifier

5.1.2. The extended state-space representation

Using Kirchoff laws and triode models, the triode stage can be modeled by a nonlinear differential algebraic system with an extended state-space representation.

The state variables are chosen according to the number of parasitic capacitances, and nonlinear functions (the plate and grid currents from the triode's

model). For the dynamic state variable X, we choose the voltages of the capacitances C_k and C_L. For the nonlinear static variable W, we choose the voltages V_{gk} and V_{pk}.

To be able to perform the coupling between this circuit and the tonestack later, we consider the input voltage V_{in} and the output current I_{out} as inputs for our system. The output voltage V_{out} and the input current I_{in} are the outputs.

$$\begin{aligned} U &= [V_{in} \quad I_{out}]^T \\ X &= [V_k \quad V_{out} - V_p]^T \\ W &= [V_p - V_k \quad V_g - V_k]^T \\ Y &= [V_{out} \quad I_{in}]^T \end{aligned} \tag{12}$$

The extended state-space representation of the system is the following :

$$f(X,W,U) = \begin{cases} (-\frac{X_1}{R_k} + I_g + I_p)/C_k \\ -\frac{X_2+W_1+X_1}{R_L C_L} + \frac{U_2}{C_L} \end{cases}$$

$$g(X,W,U) = \begin{cases} W_1 + X_1 - V_{bias} \\ \quad +R_p(I_p - U_2 + \frac{X_2+W_1+X_1}{R_L}) \\ W_2 + X_1 + \frac{R_g R_{in}}{R_g+R_{in}}(I_g - \frac{U_1}{R_{in}}) \end{cases}$$

$$h(X,W,U) = \begin{cases} X_2 + W_1 + X_1 \\ \frac{W_2+X_1-U_1}{R_{in}} \end{cases}$$

with

$$\begin{aligned} I_p &= I_p(W_1, W_2) \\ I_g &= I_g(W_1, W_2) \end{aligned} \tag{13}$$

5.1.3. Results

A sinousoid with a frequency of 200 Hz and an amplitude of 10 V feeds the input of the simulated stage. In the figure 8, the output and its harmonic content are displayed.

5.2. Tone stack

5.2.1. The circuit

Commonly found in many guitar amplifiers, the tone stack changes the frequency content of the guitar signal. The user can adjust Treble, Middle, and Bass controls to modify the gain of the respective frequency bands. The schematic is standard, and has been found in [15]. It is generally cascaded after all the preamplifier stages, and sometimes before a cathode follower.

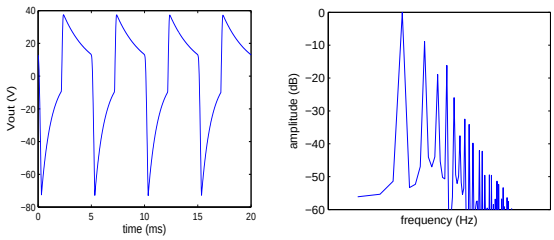

Fig. 8: Output signal

The frequency knobs are potentiometers, modeled as parameterized resistors (R_2, R_3, R_4 and R_5), with Treble, Middle and Bass controls, with values between 0 and 1.

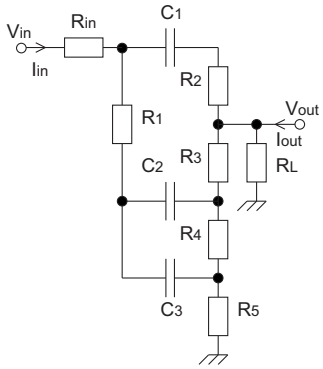

Fig. 9: The Tonestack

5.2.2. The extended state-space representation

Using Kirchoff laws, the tonestack can be modeled by a differential system with a linear state-space representation.

The state variables are the voltages of each capacitance. To be able to perform the coupling between this circuit and the tonestack later, we consider the input voltage V_{in} and the output current I_{out} as inputs for our system. The output voltage V_{out} and the input current I_{in} are the outputs.

$$\begin{aligned} U &= [V_{in} \quad I_{out}]^T \\ X &= [V_{c1} \quad V_{c2} \quad V_{c3}]^T \\ Y &= [V_{out} \quad I_{in}]^T \end{aligned} \tag{14}$$

The extended state-space representation of the system is the following :

$$f(X,U) = \begin{bmatrix} A_{11} & A_{12} & A_{13} \\ A_{21} & A_{22} & A_{23} \\ A_{31} & A_{32} & A_{33} \end{bmatrix} X + \begin{bmatrix} B_1 \\ B_2 \\ B_3 \end{bmatrix} U$$

$$h(X,U) = \begin{bmatrix} C_{11} & C_{12} & C_{13} \\ C_{21} & C_{22} & C_{23} \end{bmatrix} X + \begin{bmatrix} D_{11}D_{12} \\ D_{21}D_{22} \end{bmatrix} U$$

The expression of theses coefficients is easy to find, but a few complicated and not very relevant in this paper. For more information about tone stacks, see [4, 16].

5.2.3. Results

The frequency response of the tone stack is shown in the figure 10, for 4 different sets of knobs parameters shown, in the table 4.

	Bass	Mid	Treble
Set (1)	0.5	0.5	0.5
Set (2)	0.7	0.1	0.7
Set (3)	0.1	0.5	0.8
Set (4)	0.9	0.5	0.1

Table 4: Sets of knobs parameters

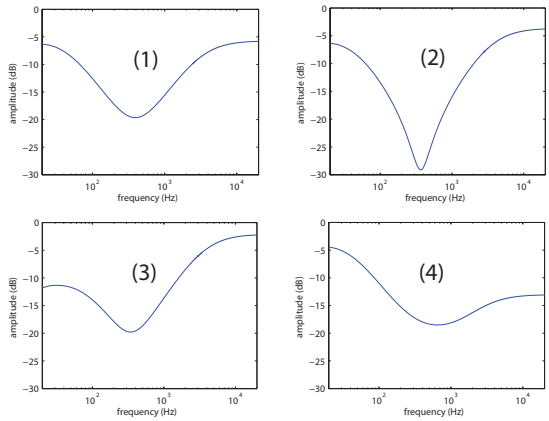

Fig. 10: The tone stack frequency's response

5.3. Coupling

With the extended state-space representation of both circuits, it is possible to simulate their combination. The components values are taken from a real preamplifier schematic. The coupling is done by adding one intermediate variable, and one equation for each relationship between one output and one input of two consecutive stages.

This preamplifier is studied in two cases, with different coupling configurations. Each time, a sinousoid with a frequency of 200 Hz and an amplitude of 1 V feeds the input of the simulated circuit. The tonestack knobs are set in an intermediate position. The output and its harmonic content are displayed in the figures 12 and 14.

Let X^{A1}, X^{A2}, X^T be the dynamic state vector of respectively the two common cathode triode amplifiers and the tonestack, W^{A1} and W^{A2} the static nonlinear states for the common cathode triode amplifiers, U^{A1}, U^{A2} and U^T the input vectors, Y^{A1}, Y^{A2}, Y^T the output vectors. The simulation of the full preamplifier is done by solving the extended state-space representation of each stage, using the numerical schemes we have seen. Moreover, some extra nonlinear static state variables W are added, to introduce the coupling relationship in the equations.

5.3.1. Stages cascaded and decoupled

First, the stages are cascaded with an imperfect coupling. The voltages are the same at the entrance and at the exit of cascaded stages, but no currents are flowing between them. This is equivalent to the following relationship :

$$\begin{aligned} Y_1^{A1} &= U_1^{A2} \\ Y_1^{A2} &= U_1^{T} \\ U_2^{A1} &= 0 \\ U_2^{A2} &= 0 \end{aligned}$$

So, the influence of cascaded stages exists only in one direction, from the input to the output of the preamplifier. The behaviour of the second triode amplifier has no influence on the behaviour of the first for example (see figure 11).

Fig. 11: Decoupled preamplifier's schematic

The equations 15 are introduced using the coupling state variables W^{A1A2} and W^{A2T}. First, we replace

some inputs in the equations with :

$$\begin{aligned} U_1^{A2} &= W^{A1A2} \\ U_1^{T} &= W^{A2T} \\ U_2^{A1} &= 0 \\ U_2^{A2} &= 0 \end{aligned}$$

Then, we introduce the outputs relationship according to the coupling variables :

$$\begin{aligned} W^{A1A2} &= X_2^{A1} + W_1^{A1} + X_1^{A1} \\ W^{A2T} &= X_2^{A2} + W_1^{A2} + X_1^{A2} \end{aligned}$$

In the extended state-space representation of the preamplifier, the dimension of the vector X is 7, and 6 for the vector W. The dimension of these vectors in each stage are added together, with the dimension of the coupling state variables for W (2).

The figure 12 displays the output and the harmonic content of the "decoupled" preamplifier.

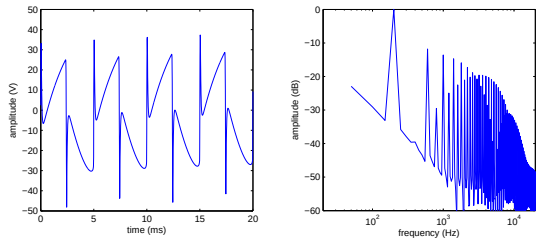

Fig. 12: Decoupled preamplifier

Note : U_2^{A2T} and Y_2^{A1A2} are not considered, because we only take account of the input and output voltages of the full preamplifiers. The input and output currents are only useful if stages exist before and after the full circuit.

5.3.2. Stages cascaded and coupled

To have a "perfect" coupling, both voltages and currents are the same at the entrance and at the exit of cascaded stages. The following relationship is introduced in the equations :

$$\begin{aligned} Y_1^{A1} &= U_1^{A2} \\ Y_1^{A2} &= U_1^{T} \\ U_2^{A1} &= Y_2^{A2} \\ U_2^{A2} &= Y_2^{T} \end{aligned}$$

The influence of cascaded stages exists in all the directions, from the input to the output of the preamplifier (see figure 13).

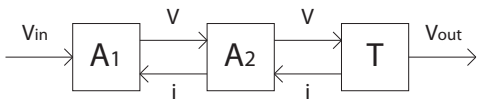

Fig. 13: Coupled preamplifier's schematic

The equations 15 are introduced using the coupling state variables W_1^{A1A2}, W_2^{A1A2}, W_1^{A2T} and W_2^{A2T}. We replace the inputs in the equations with :

$$\begin{aligned} U_1^{A2} &= W_1^{A1A2} \\ U_1^{T} &= W_1^{A2T} \\ U_2^{A1} &= W_2^{A1A2} \\ U_2^{A2} &= W_2^{A2T} \end{aligned}$$

Then, we introduce the output relationships according to the coupling variables :

$$\begin{aligned} W_1^{A1A2} &= X_2^{A1} + W_1^{A1} + X_1^{A1} \\ W_2^{A1A2} &= \frac{W_2^{A1} + X_1^{A1} - U_1^{A1}}{R_{in}} \\ W_1^{A2T} &= X_2^{A2} + W_1^{A2} + X_1^{A2} \\ W_2^{A2T} &= \begin{bmatrix} C_{21}^{A2} & C_{22}^{A2} & C_{23}^{A2} \end{bmatrix} X^{A2} \\ &\quad + \begin{bmatrix} D_{21}^{A2} D_{22}^{A2} \end{bmatrix} \begin{bmatrix} W_1^{A1A2} W_2^{A2T} \end{bmatrix}^T \end{aligned}$$

In the extended state-space representation of the preamplifier, the dimension of the vector X is 7, and 8 for the vector W. The dimension of these vectors in each stage are added together, with the dimension of the coupling state variables for W (4).

The figure 14 displays the output and the harmonic content of the "coupled" preamplifier.

6. DISCUSSION

The explicit numerical scheme of the complete stage, with different triode models, has been implemented as a real-time VST plug-in. High sampling frequencies in simulations increase the speed of the convergence of the numerical scheme, and reduce the aliasing. As a result, we have decided to choose 96 kHz as the sampling frequency.

The real triode's models have only shown a few differences, the most significant being their gain. This

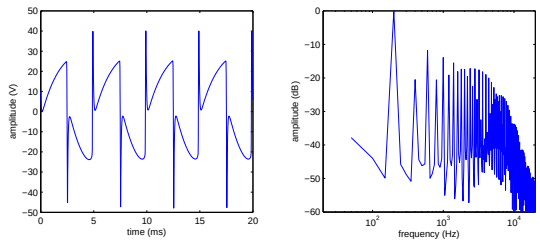

Fig. 14: Coupled preamplifier

element may not look pertinent. But a voltage decrease before a saturating triode can change a lot the harmonic response in a high gain preamplifier, with three or more triodes for example. The designers choose the polarization of each stage to get an exact quantity of saturation, without too much grid rectification. If the triode's gain changes, this parameter is no more balanced. That's why guitarists are able to tell when the preamplifier triodes become old, because they don't listen to the same quantity of saturation than before. Other remark, the interpolated (with bilinear interpolation) and estimated models of any triode give almost the same results in the simulations. But the interpolated model is prefered because it needs less CPU processing in the VST plug-in.

Then, the coupling between stages has shown to be significant. It is "imperfect" in a few market simulations to reduce the CPU consumption, but that implies a lot of loss in realism. If we compare the figures 8, 14, and 12, we can see that the preamplifier produces more distorsion than a common cathode triode amplifier alone. Nevertheless, the triode amplifier has been feed with a 10 V sinusoid in the figure 8 whereas the preamplifier has a 1V sinusoid as an input. Else, the harmonic content is different in the two coupling cases. The odd harmonics are strong in the two cases, but the coupled preamplifier shows higher even harmonics.

7. CONCLUSION

A preamplifier stage has been studied and simulated with efficient numerical schemes for real time applications. It yields to the implementation of plug-ins, which produces satisfactory sounds with standard cabinet simulations. Moreover, future work will be dedicated to model and simulate more complex topologies of guitar preamplifiers, with a larger number of triodes measured, and guitar power amplifiers.

8. REFERENCES

[1] Ivan Cohen, Thomas Helie, "Simulation of a guitar preamplifier stage for several triode models : examination of some relevant phenomena and choice of adapted numerical schemes" presented at the AES 127th convention, New York, USA, 2009.

[2] W. Marshall Leach JR., "SPICE models for vacuum tube amplifiers", in J. Audio Eng. Society, Vol. 43, No. 3, March 1995, pp. 117-126.

[3] Norman Koren, "Improved vacuum tube models for SPICE simulations", `http://www.normankoren.com`, 2003.

[4] Yeh, D. T., and J. O. Smith, "Discretization of the 59 Fender Bassman Tone Stack" in Proc. of the Int. Conf. on Digital Audio Effects (DAFx-06), New York, USA, 2006.

[5] David T. Yeh, Jyri Pakarinen, "A review of digital techniques for modeling vacuum-tube guitar amplifiers", in Computer Music Journal Summer 2009, Vol. 33, No. 2, 2009.

[6] Jean-Pierre Demailly, "Analyse numerique et equations differentielles", Collection Grenoble Sciences, 2006.

[7] Linear Technology, "LTSpice IV / SwitcherCAD III", `http://www.linear.com`, 2009

[8] Merlin Blencowe, "Designing Tube Preamps for Guitar and Bass", 2009

[9] William H. Press, Saul A. Teukolsky, William T. Vetterling, Brian P. Flannery, "Numerical Recipes in C++", Cambodge University Press, 2002

[10] J.C. Lagarias, J. A. Reeds, M. H. Wright, and P. E. Wright, "Convergence Properties of the Nelder-Mead Simplex Method in Low Dimensions", SIAM Journal of Optimization, pp. 112-147, Vol.9, no. 1, 1998

[11] De Poli Giovanni, Borin Gianpaolo and Rocchesso Davide, "Elimination of Delay-Free Loops in Discrete-Time, Models of Nonlinear Acoustic Systems", IEEE Transactions on Speech and Audio Processing, pp. 597-605, Vol. 8, no. 5, September 2000

[12] David T. Yeh and Julius O. Smith, "Simulating guitar distortion circuits, using wave digital and nonlinear state-space formulations", in Proc. of the Int. Conf. on Digital Audio Effects (DAFx-08), Espoo, Finland, Sept. 1-4, 2008.

[13] Stefano Tubaro, Francesco Santagata, Augusto Sarti, "Non-linear digital implementation of a parametric analog tube ground cathode amplifier", in Proc. of the Int. Conf. on Digital Audio Effects (DAFx-07), Bordeaux, France, 2007.

[14] Jyri Pakarinen, Matti Karjalainen, "Wave digital simulation of a vacuum-tube amplifier", in IEEE International Conference on Acoustics, Speech and Signal Processing (ICASSP06), May 2006.

[15] Duncan Amps, "Tone stack calculator", `http://www.duncanamps.com/tsc/`, Retrieved August 29th, 2010.

[16] Roman Miletitch, Ivan Cohen, Thomas Helie, "Etude et modelisation numerique d'une pedale d'effet pour guitare", master ATIAM report, 2009.